IOP Conf. Series: Materials Science and Engineering **302** (2018) 012027 doi:10.1088/1757-899X/302/1/012027

Gas Dynamic Modernization of Axial Uncooled Turbine by Means of CFD and Optimization Software

E Yu Marchukov[1] and I N Egorov[2]

[1] Chief designer, Lyulka Design Bureau, Moscow, Russia
[2] Deputy chief designer, Lyulka Design Bureau, Moscow, Russia

E-mail: egorov300657@yandex.ru

Abstract. The results of multicriteria optimization of three-stage low-pressure turbine are described in the paper. The aim of the optimization is to improve turbine operation process by three criteria: turbine outlet flow angle, value of residual swirl at the turbine outlet, and turbine efficiency. Full reprofiling of all blade rows is carried out while solving optimization problem. Reprofiling includes a change in both shape of flat blade sections (profiles) and three-dimensional shape of the blades. The study is carried out with 3D numerical models of turbines.

1. Introduction.

In the design process of turbine, the designer must ensure the number of requirements. Firstly, the turbine must have specified operation parameters (efficiency, mass flow rate, required power, etc). Secondly, turbine elements should meet the requirements of static and dynamic strength, have a predetermined life cycle and the lowest possible weight. Thirdly, parameters of LPT operation must be consistent with the parameters of the engine and parameters of other components. This means that the improvement of LPT parameters must not lead to a deterioration of the parameters of another engine components. Fourthly, the turbine must be manufacturable and have a minimum cost [1].

The development of computer technology and numerical simulation software allow to use optimization techniques in the design of turbomachinery [2-6]. Their application allows the automatic search for the optimal combination of the parameters describing the turbine design.

The goal of this study was to perform a multicriteria optimization of the three-stage LPT (Figure 1) of turboshaft engine. The following problems were addressed in course of multicriteria optimization:

1. Gas-dynamic development of LPT (operation parameters were improved) was carried out;
2. Matching the LPT with output device was improved (residual swirl after LPT was eliminated).

2. Solution algorithm for LPT optimization.

Scheme of the optimization algorithm of LPT used in the research is shown in Figure 2. At each step optimizer *IOSO PM* [3,7] generates Vector of variable parameters *x1…xn.* This vector is a set of variables that describe the geometry of turbine blade in a parametric form. The Vector is transferred to specialized programs *Profiler* [8, 9] and *Profiler 3D* convert LPT blades into geometry files (GF) in a format **.geomturbo* based on the Vector. This format is suitable for importing blade geometry in *Numeca FineTurbo*. Then, computational mesh in *Numeca AutoBlade 5* is generated using geometry

files of reprofiled LPT blades (GF1...GFn). Then, computational model is created in *Numeca FineTurbo,* and its calculation is performed. Processing of CFD results is performed in *Numeca CFView*. As a result, several output files are cre containing operation parameters of LPT (constraint vector and optimization criteria *y1*…, *yn*) in the text format. These parameters are transferred to *IOSO*, which is used for the analysis of optimization results, the selection of best results, and creation of a new vector of variable. This cycle is repeated until the desired result.

Figure 1. Three-stage LPT under optimization

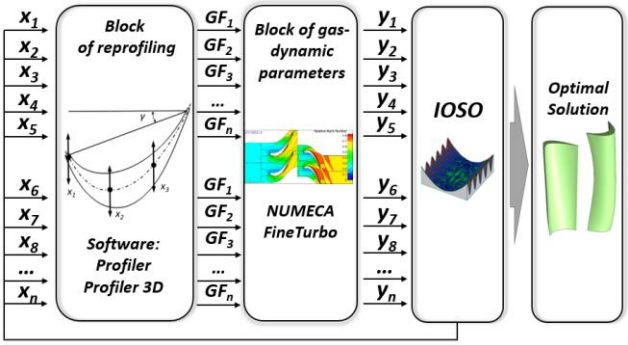

Figure 2. Optimization algorithm used in work.

Optimization procedure in *IOSO* is based on the response surface methodology [10]. Response surfaces are constructed for the objective functions and constraints. Then they are optimized at each iteration in a current search region. The objective function and constraints are then evaluated at the optimal point using the mathematical model of the system. Algorithms of *IOSO PM* have good invariant features, high level of calculation stability while optimizing the complex systems [4, 11, 12]. They also ensure the search for extremum with a presence of incompatibility areas [13, 14].

3. Development of computational model

Development of fast and accurate computational model is the most important part of optimization process (Figure 2). The computational model of turbine was created in *Numeca Auto Grid 5*. The model contained domains of inlet and outlet areas, nozzle vanes and rotor wheels. Total pressure p^*, total temperature T^*, flow angle α and turbulent viscosity were used as inlet boundary conditions. Static pressure was set at the outlet boundary [15].

Five LPT numerical models were created with different number of elements in 2D mesh of blade passage and along the height of the flow passage to perform mesh independence study [15-17] and to select the LPT mesh parameters. The first element height y+ in all created meshes was equal to 1. Parameters of created meshes are shown in Table 1.

Table 1. Basic parameters of created computational meshes of LPT.

Mesh	Number of elements in spanwise direction	Number of elements along the suction side	Number of elements along the height of blade passage	Total number of elements in 2D mesh	Total number of elements
Mesh1	43	113	57	7343	2511201
Mesh2	43	113	85	7125	3633669
Mesh3	51	141	57	10806	3695825
Mesh4	59	177	57	15780	5396545
Mesh5	75	221	57	2330	7978929

Using created computational models, the LPT characteristics were calculated: dependencies of efficiency and mass flow rate from the total pressure ration in turbine (Figure 3). From a comparison of the dependences presented in Figure 3, it was concluded:

1. Increase in the number of elements of computational model along the height (Mesh1, Mesh2) does not lead to a qualitative or quantitative change in the calculated LPT characteristics. For example, calculated values of the mass flow rate through the turbine obtained using computational meshes Mesh1 and Mesh2 differ by 0.004% (rel.), and calculated efficiency values differ by 0.001% (rel.);

2. Increase in the number of 2D mesh elements (Mesh1, Mesh4, Mesh5) lead to some quantitative change in the calculated LPT characteristics, but the qualitative nature of the dependencies does not change. As the number of elements increases, the changes in the values of calculated parameters decrease. Moreover, the mesh convergence is achieved using Mesh4. Calculated values of mass flow rate using Mesh3 and Mesh4 differ by 0.02% and by 0.008% using Mesh4 and Mesh5. Calculated values of efficiency using Mesh3 and Mesh4 differ by 0.06% and by 0.03% using Mesh4 and Mesh5.

At the next step, calculation of turbine characteristics was performed using turbulence models SA, k-ω, k-ε and computational model Mesh4 that ensured mesh convergence (Figure 4).

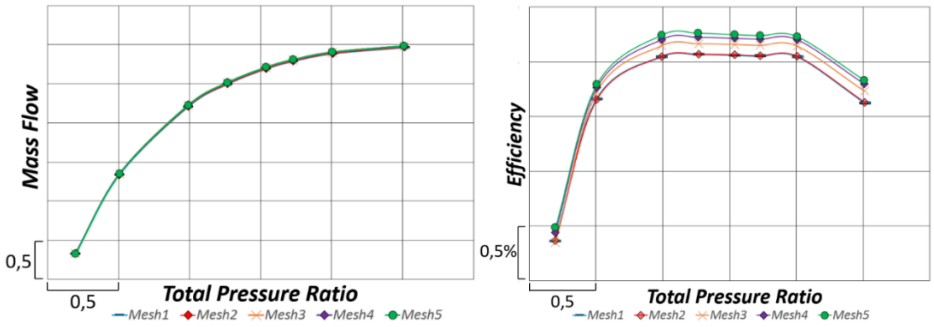

Figure 3. Comparison of LPT characteristics obtained using different models.

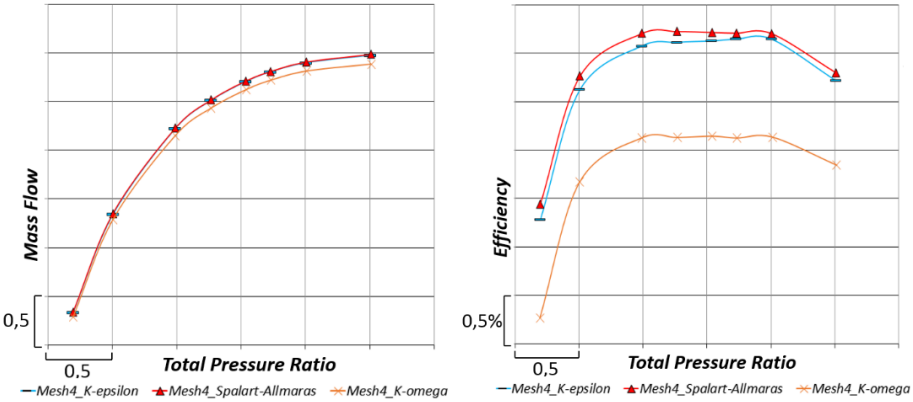

Figure 4. LPC characteristics calculated using different turbulence models.

It is clear from Figure 5 that the LPT characteristics obtained using different turbulence models qualitatively repeat each other, although there is some quantitative difference. Noteworthy is the fact that calculation results obtained using turbulence model *k-ω (Wilcox)* are significantly different from the calculation results obtained with turbulence models *Spalart-Allmaras* and *k-ε (Low Re Yang-Shih).*

Time required for the calculation was considered while selecting the turbulence model for the optimization CFD model of LPT. Calculation time with the Mesh1 on the computational node with 16 processors was 29 minutes using turbulence model *Spalart-Allmaras*, 37 minutes using turbulence model *k-ω(Wilcox)*, and 35 minutes using turbulence model *k-ε (Low Re Yang-Shih).*

Given the fact that numerical model for the optimization study should allow to capture trends in turbine operating parameters and have a minimum time of calculation in the first place, it is decided to conduct the optimization using the computational mesh with Mesh1 (2511201 elements) with *Spalart-Allmaras* turbulence model (the fastest turbulence model). Nevertheless, it is decided during the checking optimization results to use computational Mesh4 (5396545 elements), at which mesh convergence is achieved (increasing the number of elements in a mesh greater than in Mesh3 does not lead to significant differences in the value of the calculated parameters of the turbine).

4. Optimization problem statement and solution.

Gas-dynamic optimization problem was solved in three-criteria formulation with constraints.

The optimization criteria were:

1. Efficiency increase;
2. Decrease of integral flow angle at the LPT outlet α_{out} (Figure 5). It must not be less than 15°;
3. Decrease of the residual flow swirl $\Delta\alpha_{out}$ at the outlet of LPT (Figure 5). It must be not greater than 10°.

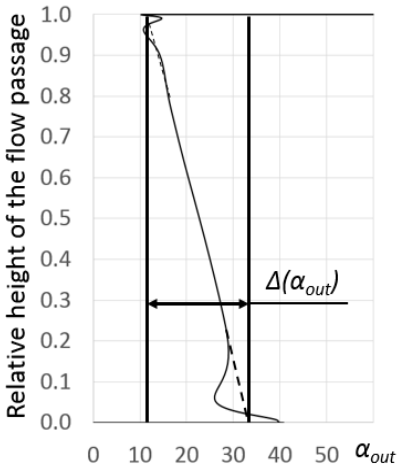

Figure 5. Parameters $\boldsymbol{\alpha_{out}}$ and $\boldsymbol{\Delta\alpha_{out}}$.

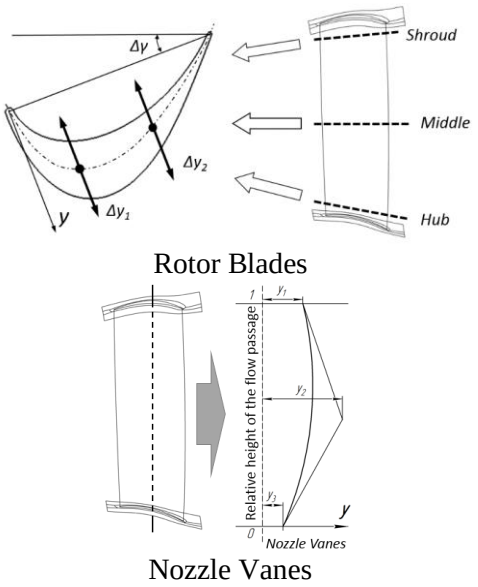

Figure 6. Scheme of variables of gas dynamic optimization problem of LPT.

Constraints for gas dynamic optimization were: mass flow rate *G*, expansion ratio π_T^*, power *N*. These parameters must not be changed during optimization by more than 0.5% relatively to the values of base LPT.

Geometric parameters of rotor blades and nozzle guide vanes were used as variables in gas-dynamic optimization. 2D and 3D reprofiling was performed for all nozzle vanes of LPT. Only 2D reprofiling was done for all rotor blades.

2D reprofiling of nozzle vanes and rotor blades was carried out by changing stagger angles of profile γ and ordinates of midpoints of spline Δy1 and Δy2 in three sections (hub, middle and shroud, Figure 6). The total number of variables for 2D reprofiling was 9 per blade.

3D reprofiling of nozzle vanes was performed by circumferential and axial shifts of the sections, and by scaling the chord of sections. Variation of these parameters along the height of the flow passage was described by Bezier curve with 3 control points (Figure 6). The values of ordinates of 3 control points were changed during optimization. The number of variables used for 3D reprofiling of nozzle vanes was 9 per blade. Total number of variables in the gas-dynamic optimization was 81. Solution of the optimization problem took nearly 1,000 iterations with computational model.

Pareto front was obtained during the optimization for the value of integral flow angle at the outlet of LPT α_{out}, residual swirl $\Delta\alpha_{out}$ and efficiency (Figure 7). The efficiency in the figure is presented not as an absolute value, but as an efficiency drop ΔEff_i relatively the efficiency of the base LPT variant.

$$\Delta Eff_i = Eff_{Base} - Eff_i \quad (1)$$

where Eff_{Base} – the value of efficiency of base LPT variant; Eff_i – the value of efficiency of i-variant of LPT from Pareto set.

The value of ΔEff_i is shown in Figure 7 as circles. The greater the diameter of the circle is, the greater the ΔEff_i relatively the efficiency of the base LPT variant.

It should be noted that unique geometry of LPT corresponds to every point of Pareto.

Analysis of Pareto front showed that decrease in flow angle α_{out} and residual swirl $\Delta\alpha_{out}$ is followed by efficiency drop. At the same time, minimal efficiency drop is 0.12% and it is achieved with virtually extreme (in terms of optimization constraints) values of α_{out} and $\Delta\alpha_{out}$ (Table 2).

Four points of Pareto set were selected for the further analysis:

1. Point with the minimal value of efficiency drop relatively to the base variant (Variant 1);
2. Point with the minimal value of flow angle at the LPT outlet α_{out} (Variant 2);
3. Point with the minimal value of flow swirl at the LPT outlet $\Delta\alpha_{out}$ (Variant 3);
4. Compromise point (Variant 4).

Values of LPT parameters in selected points of Pareto front are shown in Table 2. Verification of the results of LPT gas-dynamic optimization was performed with Mesh4 as the finest mesh.

Table 2. The values of LPT parameters in the selected points of the Pareto front.

LPT variant	Efficiency drop, $\Delta\boldsymbol{Eff}_i$, %	Outlet flow angle $\boldsymbol{\alpha_{out}}$, degree	$\boldsymbol{\Delta\alpha_{out}}$, degree
Base	0	22.73	12.79
Variant 1	0.12	14.92	9.89
Variant 2	0.386	9.82	9.92
Variant 3	0.292	14.95	3.06
Variant 4	0.262	13.53	4.83

Figure 8 shows the graphs of distribution of the flow angle in absolute motion at the outlet of LPT along the height of flow passage for 4 selected LPT variants compared to the base case. It should be noted that the parameters α_{out} and $\Delta\alpha_{out}$ were significantly decreased.

Figure 9 shows a comparison of Mach numbers, averaged in the circumferential direction for some LPT variants compared to the base one. The main changes in the flow structure occurred in the latest stage. Comparison of the blade shapes of the base and the final LPT variants is shown in Figure 10.

Thus, the outlet angle and the residual swirl value of the flow in the outlet section of the turbine were set to the required range, although this was achieved by some drop in efficiency (Table 2).

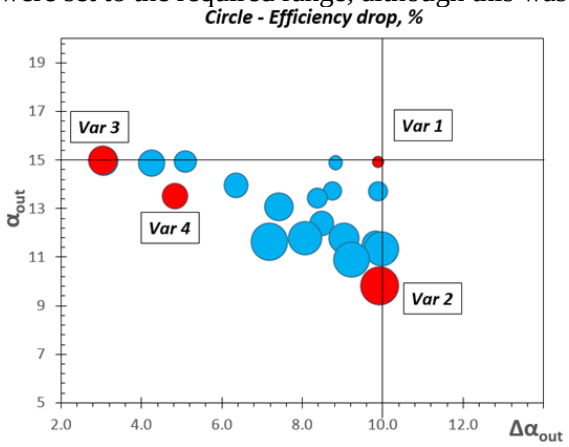

Figure 7. The Pareto Set.

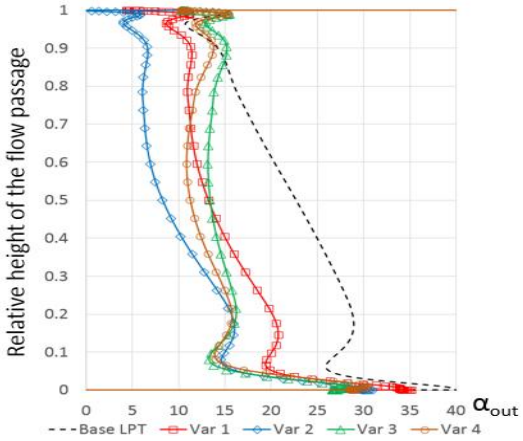

Figure 8. Outlet flow angle in absolute motion along the height of flow passage.

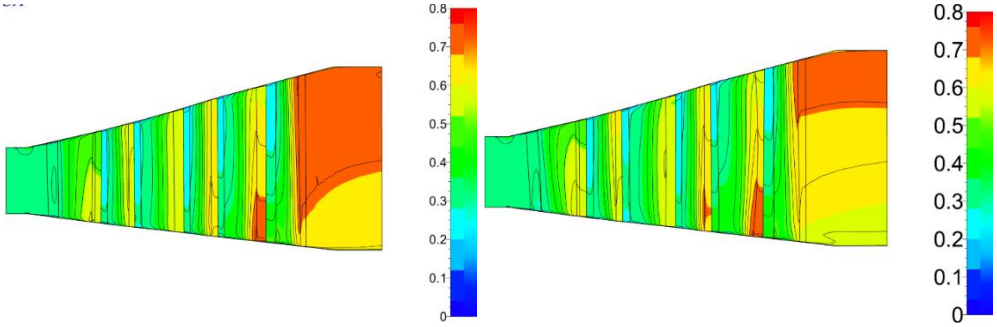

Base variant of LPT *LPT Variant 1*

Figure 9. Comparison of the Mach number in the flow passage of the LPT for different variants.

5. Conclusion

Five numerical models of LPT with different density of computational mesh were created. All these models allow predicting the trend of the LPT characteristics, but they give a quantitative difference in the calculated parameters.

The model Mesh1 with turbulence model Spalart-Allmaras provides the shortest calculation time of one point of LPT characteristics. At the same time, it allows predicting the LPT characteristics and can be used for optimization studies. Mesh4 was used for the final check of the obtained results as the most accurate mesh.

During the optimization, new LPT variants were found. They provide a decrease in the average value of the outlet angle by 12.9 degrees, as well as a decrease in the residual flow swirl at the turbine outlet by 9.8 degrees. These changes are possible due to some drop of efficiency (0.12%).

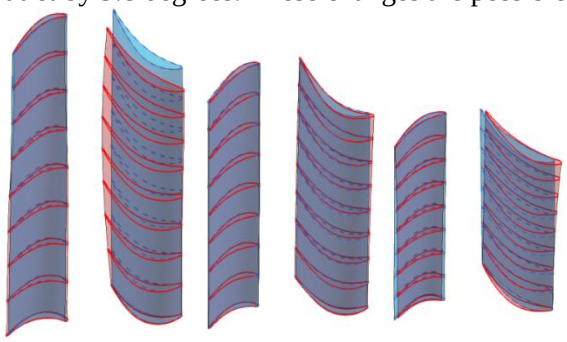

Figure 10. Comparison of the blade geometry of base and optimized LPT variants (blue blades - basic LPT, red blades - optimized LPT)

References

[1] Von Karman Institute for Fluid Dynamics, Aero-engine Design: From State of the Art Turbofans Towards Innovative Architectures, Lecture Series 2008-03.
[2] Inozemcev A A 2008 *Osnovy Konstruirovaniya Aviacionnyh Dvigatelej i Ehnergeticheskih Ustanovok (Fundamentals of Aircraft Engines and Power Plants Designing)* (Mashinostroenie, Moskow) p 366
[3] Egorov I N, Kretinin G V, Leshchenko I A, Kuptzov S V 2002 *9th AIAA/ISSMO Symposium on Multidisciplinary Analysis and Optimization* Code 103018
[4] Matveev V N, Popov G M, Baturin O V, Goryachkin E S and Kolmakova D A 2015 *51st AIAA/SAE/ASEE Joint Propulsion Conf.* Code 130539
[5] Khairuddin U, Costall A W and Martinez-Botas R F 2015 *Proc. of the ASME Turbo Expo* Paper No. GT2015-42053.
[6] Buske, C., Krumme, A., Schmidt, T., Dresbach, C., Zur, S. ,Tiefers, R, 2016 *Proc. of the ASME Turbo Expo* Paper No.GT2016-56079
[7] IOSO Optimization Technology. Access mode: http://www.iosotech.com.
[8] Shabliy L S and Dmitrieva I B 2014 *ARPN J. of Engineering and Applied Sciences* 9 (10) 1849-53
[9] Shabliy L S and Dmitrieva I B *Russian Aeronautics* pp 276-82
[10] Dennis B H, Egorov I N, Dulikravich G S and Yoshimura S 2003 *American Society of Mechanical Engineers, International Gas Turbine Institute, Turbo Expo (Publication) IGTI* GT2003-38051
[11] Popov G, Goriachkin E, Kolmakova D and Novikova Y 2016 *Proc. of the ASME Turbo Expo* Paper No. GT2016-57856
[12] Baturin O V, Popov G M, Goryachkin E S and Novikova Y D 2015 *5th Int. Conf. on Simulation and Modeling Methodologies, Technologies and Applications, Proc.* Pp 227-32
[13] Ivachnenko A G 1982 *Inductive method of selforganization for complex systems models* (Kiev, Naukova Dumka)

[14] Egorov I N and Kretinin G V 1996 *World Publishing Corporation, Aerothermo-dynamics of internal flows III* (Beijing, China) pp 112-20
[15] Popov G, Goryachkin E, Baturin O and Kolmakova D 2014 *Int. J. of Engineering and Technology* 6(5) 2236-43
[16] Abraham S, Panchal K, Ekkad S V, (...), Brown B J and Malandra A 2011 *Proc. of the ASME Turbo Expo* Paper No. GT2011-45188
[17] Macisaac G D, Sjolander S A, Praisner T J, Grover E A and Jurek R 2013 *Proc. of the ASME Turbo Expo* Paper No. GT2013-95670